directly measure such a rate constant with the LIF technique. However, our results, as well as those of Sanders et al. [4], indicate a slower rate for methoxy removal by CO in this temperature range.

The curvature in the Arrhenius plot (fig. 3) may indicate the onset, at increasing temperatures, of another mechanism for methoxy removal by CO. One such mechanism may be the reaction of methoxy with CO to produce the formyl radical and formaldehyde, i.e.

$$CH_3O+CO\rightarrow HCO+CH_2O\,. \qquad (2)$$

Thermochemical calculations for reactions (1) and (2), using the enthalpies of formation tabulated by Okabe [11], show that reaction (1) is thermodynamically favored (exothermic, $\Delta H=-35$ kcal $mol^{-1}$) over an approximately thermoneutral reaction (2). To the extent that this reaction is important, one should observe either $CH_2O$ as a product as well as $CH_3OH$. As noted before, Lissi et al. [2] observed that neither $CH_2O$ nor the further reaction product $CH_3OH$ were detectable in their system. Consequently, reaction (2) is probably not an important methoxy removal channel in the 396–426 K range. However, this result does not preclude the increased importance of reaction (2) at our higher temperatures.

Sæbø, Radom and Schaefer [12] predict that decomposition of $CH_3O$ to $CH_2O$ and H requires an activation energy of 34.4 kcal $mol^{-1}$ while isomerization to $CH_2OH$ has an activation energy of 36 kcal $mol^{-1}$. Thus, at elevated temperatures, collision-induced decomposition of $CH_3O$ by the reaction

$$CH_3O+CO\rightarrow CH_2O+H+CO\,, \qquad (3)$$

or isomerization of $CH_3O$ via the reaction

$$CH_3O+CO\rightarrow CH_2OH+CO \qquad (4)$$

may also represent important methoxy removal channels.

The results presented in this paper would seem to indicate that at least two removal channels for $CH_3O+CO$ are important. Currently, it is not possible to distinguish between the different channels. Studies of reactions of $CH_3O$ with non-reactive species such as argon, nitrogen, and $CF_4$ are currently in progress in our laboratory. Such studies will help to ascertain the importance of reactions (3) and (4). Preliminary measurements for methoxy removal by such unreactive collision partners indicate that processes like (3) and (4) can be quite important at elevated temperatures. However, further experiments and analysis are required to fully deconvolute the fundamental rate constant parameters for the reaction of $CH_3O$ with CO.

## Acknowledgement

This work was supported by the Morgantown Energy Technology Center (DOE) and was performed under the auspices of the Department of Energy. PJW gratefully acknowledges the support provided by the LANL Photochemistry and Photophysics Group (CLS-4) during his postdoctoral appointment.

## References

[1] W. Tsang and R.F. Hampson, J. Phys. Chem. Ref. Data 15 (1986) 1087.
[2] E.A. Lissi, G. Massiff and A.E. Villa, J. Chem. Soc. Faraday Trans. I 69 (1973) 346.
[3] H.A. Wiebe and J. Heicklen, J. Am. Chem. Soc. 95 (1973) 1.
[4] N. Sanders, J.E. Butler, L.R. Pasternack and J.R. McDonald, Chem. Phys. 48 (1980) 203.
[5] G. Inoue, H. Akimoto and M. Okuda, J. Chem. Phys. 72 (1980) 1769.
[6] W. Felder, A. Fontijn, H.N. Volltrauer and D.R. Voorhees, Rev. Sci. Instr. 51 (1980) 195.
[7] S.L. Baughcum and R.C. Oldenborg, in: The chemistry of combustion processes, ed. Th. M. Sloane, Am. Chem. Soc. Symp. Series, No. 259 (Am. Chem. Soc., Washington, 1984) pp. 257–266.
[8] P.J. Wantuck, R.C. Oldenborg, S.L. Baughcum and K.R. Winn, J. Phys. Chem, to be published.
[9] L. Batt, R.T. Milne and R.D. McCulloch, Intern. J. Chem. Kinetics 9 (1977) 567.
[10] E.A. Arden, L. Phillips and R. Shaw, J. Chem. Soc. (1964) 5126.
[11] H. Okabe, Photochemistry of small molecules (Wiley, New York, 1978) pp. 375–380.
[12] S. Sæbø, L. Radom and H.F. Schaefer III, J. Chem. Phys. 78 (1983) 845.





# EXPERIMENTAL SEPARATION OF TORSIONAL AND CHARGE REDISTRIBUTION EFFECTS IN ROTATIONAL SPECTRA OF HCN DIMERS

R.S. RUOFF, T. EMILSSON, C. CHUANG, T.D. KLOTS and H.S. GUTOWSKY
*Noyes Chemical Laboratory, University of Illinois, Urbana, IL 61801, USA*

Received 24 March 1987; in final form 11 May 1987

$B_0$ and $D_J$ have been determined for $H^{13}C^{15}N$–$HC^{15}N$, $HC^{15}N$–$H^{13}C^{15}N$, $HC^{15}N$–$DC^{14}N$ and $DC^{14}N$–$HC^{15}N$. From them and other, previous results a full substitution structure has been obtained for HCN(1)–HCN(2). It leads to torsional amplitudes $\theta_1$ and $\theta_2$ of 13.6 and 9.3° for the two monomers in the dimer. A determination by fitting $B_0$ for six isotopic species gives 13.7 and 8.7°. These values are used to separate torsional and charge redistribution effects upon the hyperfine interactions of $^{14}N$ and D in the dimers. For $^{14}N$, about 40% of the difference in $\chi_a$ between HCN monomer and dimer is caused by charge redistribution. The C–D bond length in the dimer is considered.

## 1. Introduction

A large number of hydrogen-bonded dimers has been studied by a variety of experimental and theoretical techniques. Recently, we have determined the rotational constants of several hydrogen-bonded trimers which contain the HCN dimer as a subunit[#1], including the HCN trimer. Analysis of our results for these trimers is furthered by a better understanding of the related properties for the HCN dimer. In particular, we need a sound basis for determining the torsional amplitudes and distances between the monomer units in the trimers. Also, information is sought about the electronic interactions governing the structures of the trimers.

The HCN dimer is known to have a linear equilibrium structure because *l*-type doubling has been observed in its degenerate bending vibration [2]. Rotational and centrifugal distortion constants $B_0$ and $D_J$ have been reported for the four $^{14}N/^{15}N$ isotopic species of the $H^{12}CN$ dimer [3] and the three (additional) species of $(H/D^{12}C^{15}N)_2$ [4]. Also, hyperfine interaction constants $\chi_a$ were obtained for the dimers containing $^{14}N$ and D. The model typically employed to relate $B_0$ to the distance between linear monomer units in a dimer with torsionally averaged axial symmetry (fig. 1) is

$$I_b^{\mathrm{d}}=\mu R^2+\tfrac{1}{2}\langle 1+\cos^2\theta_1\rangle I_1^{\mathrm{m}}$$
$$+\tfrac{1}{2}\langle 1+\cos^2\theta_2\rangle I_2^{\mathrm{m}}\,. \qquad (1)$$

$I_b^{\mathrm{d}}$ is the moment of inertia about the *b* axis of the dimer, $\mu$ is the reduced mass of the dimer viewed as diatomic, $R$ is the distance between the centers of mass (c.m.) of the monomers and $I_n^{\mathrm{m}}$ is the moment of inertia for the *n*th monomer. The torsional angles $\theta_1$ and $\theta_2$ can be operationally defined by projection onto the *a* axis of the hyperfine interaction for a

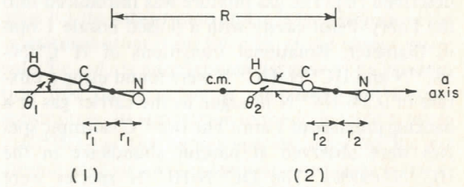


Fig. 1. Geometrical structure and coordinates of the HCN dimer. Atomic positions are to scale. The center of mass of the dimer is at c.m.; the other dots on the *a* axis are the c.m. of the monomers.

[#1] They are HCN–HCN–X with X = HCN, HF, HCl and $HCF_3$, and Y–HCN–HCN with Y = $H_3N$, $N_2$, OC, ethylene, cyclopropane, $H_2O$ and $CO_2$. For a preliminary account of the results for the HCN trimer, see ref. [1].

nucleus in each of the monomers, such as

$$\chi_a = \tfrac{1}{2}\langle 3\cos^2\theta - 1\rangle \chi_0^{\mathrm{d}} \qquad (2)$$

where $\chi_0^{\mathrm{d}}$ is the quadrupole interaction constant for the rigid, linear dimer.

The attraction in rare gas–DX dimers is weak enough that dimer formation does not make $\chi_0^{\mathrm{d}}(\mathrm{D})$ differ significantly from the free monomer value $\chi_0^{\mathrm{m}}$ [5]. The latter can then be used in eq. (2) with the observed $\chi_a$ to obtain reliable values for $\theta$. Application of this approach to the $\chi_a(^{14}\mathrm{N})$ found in the $^{14}\mathrm{N}/^{15}\mathrm{N}$ HCN dimers gives values of 17.0 and 11.4° for $\theta_1$ and $\theta_2$, respectively. However, a theoretical analysis indicates that the strong hydrogen bonding in these dimers causes charge rearrangement producing approximately half of the observed differences $\Delta\chi_a$ between the $\chi_a$ and $\chi_0^{\mathrm{m}}(\mathrm{HC}^{14}\mathrm{N})$ [3]. A more accurate experimental separation of torsional and charge rearrangement effects can be based on moments of inertia for several isotopic species, provided the torsional angles and intermonomer distance are insensitive to the substitution employed or allowance can be made for the changes. This report describes such an approach. It includes determination of $B_0$, $D_J$, $\chi_a(\mathrm{D})$ and $\chi_a(^{14}\mathrm{N})$ for some additional isotropic species employed in the analysis, namely the two $^{13}\mathrm{C}$ monosubstituted dimers of $\mathrm{HC}^{15}\mathrm{N}$ and the two dimers of $\mathrm{DC}^{14}\mathrm{N}$ with $\mathrm{HC}^{15}\mathrm{N}$.

## 2. Experimental

The rotational transitions of these four dimers were observed with the Flygare/Balle Mark II, pulsed Fourier transform microwave spectrometer, which has been modified extensively to enhance performance. Details of spectrometer operation have been described [6]. The gas mixture was introduced into the Fabry–Pérot cavity with a pulsed nozzle 1 mm in diameter. Rotational transitions of $\mathrm{H}^{13}\mathrm{C}^{15}\mathrm{N}$–$\mathrm{HC}^{15}\mathrm{N}$ and $\mathrm{HC}^{15}\mathrm{N}$–$\mathrm{HC}^{15}\mathrm{N}$ were found using a mixture of 0.3% $\mathrm{HC}^{15}\mathrm{N}$ in argon as the carrier gas at a backing pressure of 1 atm. The two $^{13}\mathrm{C}$ isotropic species were observed at natural abundance in the $\mathrm{HC}^{15}\mathrm{N}$ (99%). The $\mathrm{DC}^{14}\mathrm{N}/\mathrm{HC}^{15}\mathrm{N}$ species were observed by using a 1:1 mixture of $\mathrm{HC}^{15}\mathrm{N}$ and $\mathrm{DC}^{14}\mathrm{N}$ at a total concentration of about 0.3% in argon at 1atm. The $\mathrm{HC}^{15}\mathrm{N}$ was made by addition of orthophosphoric acid to $\mathrm{KC}^{15}\mathrm{N}$ (Cambridge Isotope Laboratories). The $\mathrm{DC}^{14}\mathrm{N}$ was made by addition of deuterated orthophosphoric acid to KCN.

## 3. Results

The line centers found for the four dimers are listed in table 1. Our primary interest was to determine the $B_0$ for use in the structural analysis. The $\mathrm{H}^{13}\mathrm{C}^{15}\mathrm{N}/\mathrm{HC}^{15}\mathrm{N}$ dimers have no hyperfine structure (hfs). Frequencies were measured for their $J=1\rightarrow2$ and $2\rightarrow3$ transitions and fitted to determine $B_0$ and $D_J$. The $\mathrm{DC}^{14}\mathrm{N}/\mathrm{HC}^{15}\mathrm{N}$ dimers have hfs from quadrupole coupling of the D as well as the $^{14}\mathrm{N}$. It was observed for the $J=0\rightarrow1$ transitions and fitted by full matrix diagonalization in the coupled basis

$$J+I_{\mathrm{D}}=F_1, \quad F_1+I_{\mathrm{N}}=F\,. \qquad (3)$$

The least-squares fit did not converge readily when both $\chi_a(\mathrm{D})$ and $\chi_a(^{14}\mathrm{N})$ were adjustable parameters. Therefore, a grid search was employed to find the approximate minimum. The parameters for it were used as input values for a fit which then converged. The resulting fit of the observed hfs is given in table 2 and the values found for $\chi_a(^{14}\mathrm{N})$ and $\chi_a(\mathrm{D})$ in table 3. $D_J$ for the dimers is only $\approx 2$ kHz so it was assigned by reference to similar, observed $B_0$, $D_J$ pairs. Thereby, $B_0$ was obtained for the two $\mathrm{DC}^{14}\mathrm{N}/\mathrm{HC}^{15}\mathrm{N}$ dimers from their $J=0\rightarrow1$ line centers. The results for $B_0$ and $D_J$ of the four dimers are included in table 3 along with the values reported earlier for other HCN dimers, including the measurements of $\chi_a$.

Table 1
Line centers observed for four isotopic species of the HCN dimer

| Isotopic species | Transition $J\rightarrow J'$ | Observed (MHz) |
|---|---|---|
| $\mathrm{H}^{13}\mathrm{C}^{15}\mathrm{N}$–$\mathrm{HC}^{15}\mathrm{N}$ | 1→2 | 6568.984(2) |
| | 2→3 | 9853.361(2) |
| $\mathrm{HC}^{15}\mathrm{N}$–$\mathrm{H}^{13}\mathrm{C}^{15}\mathrm{N}$ | 1→2 | 6677.199(2) |
| | 2→3 | 10015.680(2) |
| $\mathrm{HC}^{15}\mathrm{N}$–$\mathrm{DC}^{14}\mathrm{N}$ | 0→1 | 3457.1465(2) |
| $\mathrm{DC}^{14}\mathrm{N}$–$\mathrm{HC}^{15}\mathrm{N}$ | 0→1 | 3238.1476(6) |





Table 2
Observed and calculated frequencies for the hyperfine components of the $J=0\rightarrow1$ transitions of the $\mathrm{HC}^{15}\mathrm{N}/\mathrm{DC}^{14}\mathrm{N}$ dimers

| | Transition $J,F_1,F\rightarrow J',F_1',F'$ | Observed (MHz) | Calculated (MHz) | Difference (kHz) |
|---|---|---|---|---|
| $\mathrm{HC}^{15}\mathrm{N}$–$\mathrm{DC}^{14}\mathrm{N}$ | 0,1,2→1,1,1 | 3456.0090 | 3456.0093 | −0.3 |
| | 0,1,2→1,2,2 | 3456.0383 | 3456.0379 | 0.4 |
| | 0,1,0→1,0,1 | 3457.3383 | 3457.3389 | −0.6 |
| | 0,1,2→1,2,3 | 3457.3611 | 3457.3601 | 1.0 |
| | 0,1,1→1,1,2 | 3457.4002 | 3457.4008 | −0.6 |
| | 0,1,2→1,2,1 | 3459.3728 | 3459.3727 | 0.1 |
| $\mathrm{DC}^{14}\mathrm{N}$–$\mathrm{HC}^{15}\mathrm{N}$ | 0,1,2→1,1,1 | 3237.0861 | 3237.0854 | 0.7 |
| | 0,1,2→1,2,2 | 3237.1170 | 3237.1162 | 0.8 |
| | 0,1,0→1,0,1 | 3238.3210 | 3238.3227 | −1.7 |
| | 0,1,2→1,2,3 | 3238.3454 | 3238.3451 | 0.3 |
| | 0,1,1→1,1,2 | 3238.3877 | 3238.3887 | −1.0 |
| | 0,1,2→1,2,1 | 3240.2208 | 3240.2198 | 1.0 |

Table 3
Rotational constants determined for the HCN dimers

| Isotopic species | $B_0$ (MHz) | $D_J$ (kHz) | HCN(1) | | HCN(2) | | Ref. |
|---|---|---|---|---|---|---|---|
| | | | $\chi_{\mathrm{D}}$ (kHz) | $\chi_{\mathrm{N}}$ (MHz) | $\chi_{\mathrm{D}}$ (kHz) | $\chi_{\mathrm{N}}$ (MHz) | |
| $\mathrm{HC}^{14}\mathrm{N}$–$\mathrm{HC}^{14}\mathrm{N}$ | 1745.8097(5) | 2.133(30) | – | −4.0973(200) | – | −4.4400(190) | [3] |
| $\mathrm{HC}^{14}\mathrm{N}$–$\mathrm{HC}^{15}\mathrm{N}$ | 1700.3019(3) | 1.939(40) | – | −4.1059(10) | – | – | [3] |
| $\mathrm{HC}^{15}\mathrm{N}$–$\mathrm{HC}^{14}\mathrm{N}$ | 1729.9208(2) | 2.023(30) | – | – | – | −4.4339(6) | [3] |
| $\mathrm{HC}^{15}\mathrm{N}$–$\mathrm{HC}^{15}\mathrm{N}$ | 1684.2882(3) | 1.900(30) | – | – | – | – | [3] |
| $\mathrm{DC}^{15}\mathrm{N}$–$\mathrm{HC}^{15}\mathrm{N}$ | 1605.6946(1) | 1.684(4) | 182.9(14) | – | – | – | [4] |
| $\mathrm{HC}^{15}\mathrm{N}$–$\mathrm{DC}^{15}\mathrm{N}$ | 1683.3736(2) | 1.885(5) | – | – | 175.6(16) | – | [4] |
| $\mathrm{DC}^{15}\mathrm{N}$–$\mathrm{DC}^{15}\mathrm{N}$ | 1604.4947(6) | 1.64(1) | – | – | – | – | [4] |
| $\mathrm{H}^{13}\mathrm{C}^{15}\mathrm{N}$–$\mathrm{HC}^{15}\mathrm{N}$ | 1642.2613(9) | 1.91(6) | – | – | – | – | a) |
| $\mathrm{HC}^{15}\mathrm{N}$–$\mathrm{H}^{13}\mathrm{C}^{15}\mathrm{N}$ | 1669.3155(9) | 1.98(6) | – | – | – | – | a) |
| $\mathrm{HC}^{15}\mathrm{N}$–$\mathrm{DC}^{14}\mathrm{N}$ | 1728.577 | 2.02 [b] | – | – | 179.2(55) | −4.4509(25) | a) |
| $\mathrm{DC}^{14}\mathrm{N}$–$\mathrm{HC}^{15}\mathrm{N}$ | 1619.076 | 1.69 [b] | 191.6(55) | −4.1426(25) | – | – | a) |

[a] This work. [b] Obtained as described in section 3.

## 4. Separation of torsional and charge redistribution effects

### 4.1. Substitution structure

A full substitution structure can be obtained for the HCN dimer from the $B_0$ values now available. For a linear molecule, substitution of a particular atom by an isotope is described by the approximate equation [7]

$$I_{\mathrm{B}'} = I_{\mathrm{B}} + \mu_{\mathrm{s}} a_i^2\,, \qquad (4)$$

where $I_{\mathrm{B}'}$ is the moment of inertia for the new species, $I_{\mathrm{B}}$ is that of the parent molecule, $\mu_{\mathrm{s}}$ is the reduced mass for the substitution and $a_i$ is the distance of the substituted atom from the c.m. of the parent molecule. Eq. (4) is approximate because of its assumption that the structure is unchanged by isotopic substitution. Its application to the $B_0$ in table 3, using $(\mathrm{HC}^{15}\mathrm{N})_2$ as the parent species, leads to the six atomic positions and interatomic distances given in table 4. A conversion factor of 505379.0 amu Å$^2$ MHz was used for $I_{\mathrm{B}}B_0$.

The atomic positions are averaged over the zero-

Table 4
Substitution positions and interatomic distances determined for the HCN dimer [a]

| Atom | Position (Å) | Atomic species | Distance (Å) |
|---|---|---|---|
| H(1) | −3.8545 | C–H(1) | 1.0634 |
| C(1) | −2.7911 | C–N(1) | 1.1226 |
| N(1) | −1.6685 | C–H(2) | 1.2463 |
| H(2) | 0.4061 | C–H(2) | 1.1399 |
| C(2) | 1.6524 | C(1)...C(2) | 4.4435 |
| N(2) | 2.7923 | N(1)...N(2) | 4.4608 |

[a] Based on $B_0$ values in table 3 with $(HC^{15}N)_2$ as the parent species.

point vibrations of the dimer, the largest of which is most likely the axially symmetric torsional oscillation of the monomers. Therefore, as shown in fig. 1, the positions determined are the projections onto the $a$ axis of nuclei strung along the relatively rigid monomer. The C–N distance in the monomer, $r^m$(C–N) is projected by $\langle\cos\theta_n\rangle$ into the smaller value $r_s^d$(C–N) for the dimer; that is [8]

$$r_s^d(\text{C–N}) = r^m(\text{C–N})\langle\cos\theta_n\rangle\,. \tag{5}$$

Substitution of the $a_i$ for the C and N in the two subunits of the dimer give $r_s^d$(C–N) to be 1.1226 and 1.1399 Å for monomers 1 and 2, respectively (table 3). The reported $r_s^m$ value for the C–N distance in HCN monomer is 1.15512(16) [9], a value which probably is not affected appreciably by dimer formation. With this assumption, eq. (5) gives $\theta_1$ and $\theta_2$ to be 13.6 and 9.3°, where $\theta_n$ is operationally defined as arc$\langle\cos\theta_n\rangle$. This definition of $\theta$ differs negligibly from that of eq. (2).

In principle, the same approach could be applied to the C–H bond distance. However, the substitution method is unreliable for atoms close to the c.m. and H(2) is only ≈0.4 Å from it. The error in the H(2) position is evident in the $r_s$ result of 1.25 Å for C–H(2), which is impossibly long. A further complication is that the C–D bond in the monomer is shorter than the C–H, as discussed in section 4.4.

*4.2. Inertial analysis*

A somewhat different method for estimating $\theta_1$ and $\theta_2$ is based upon eq. (1) for the moment of inertia of the isotopic dimers. Eq. (1) contains three unknowns: $\theta_1$, $\theta_2$ and $R$. Of these, the $\theta$ are insensitive to isotopic substitution. For two isotopic species of the monomer, one has $\theta_{ni}/\theta_{nj} \approx (I_j^m/I_i^m)^{1/4}$, so $^{14}N/^{15}N$ or $^{12}C/^{13}C$ substitution changes $\theta_n$ by a factor of only ≈ 1.007, which we ignore. However, isotopic substitution in a monomer changes the position of its c.m. and affects $R$, the c.m. separation in the dimer, by (fig. 1)

$$R = R_C - r_1' + r_2' = R_N + r_1 - r_2\,, \tag{6}$$

where

$$r_n' = r_C\langle\cos\theta_n\rangle \quad\text{and}\quad r_n = r_N\langle\cos\theta_n\rangle\,. \tag{7}$$

The quantities $r_C$ and $r_N$ are the distances within a given monomer between the C or N and the monomer's c.m. They were calculated using the $r_s$ distances 1.06314(11) and 1.15512(16) Å for the C–H and C–N bond lengths [9]. $R_C$ and $R_N$ are the distances along the $a$ axis between the projected positions of the two nitrogens and the two carbons, respectively; they are taken to be independent of isotopic substitution. If $\theta_1 = \theta_2$, then for a homonuclear dimer $R = R_C = R_N$, while if $\theta_1 > \theta_2$, then $R_N > R_C$, as observed (table 4).

Eqs. (1), (6) and (7) were used to fit the $B_0$ determined for the dimers, with $\theta_1$, $\theta_2$ and $R_C$ or $R_N$ treated as the adjustable parameters. In eq. (1), the values adopted for $I^m$ were those observed for the particular monomers [9]. By fitting the four $B_0$ values at the top of table 3 for the $^{14}N/^{15}N$ species and the two near the bottom for (13,15)–15 and 15–(13,15) we obtained values of 13.7 and 8.7° for $\theta_1$ and $\theta_2$ and 4.43788 and 4.45748 Å for $R_C$ and $R_N$. These results fit the $B_0$ values with an rms deviation of 25 kHz. The value for $R$ depends of course on the isotopic species. Our model implies that $R$ should be equal in the 14–14 and 15–15 homonuclear dimers, while the analysis gives 4.44735 and 4.44771 Å, respectively. Limiting the fit to the first four or the last three $B_0$ values of the six used does not affect the results materially.

The values of 13.7 and 8.7° found in this way for $\theta_1$ and $\theta_2$ compare favorably with the 13.6 and 9.3° from the substitution structure. It is noteworthy however that the substitution values for $R_C$ and $R_N$ are somewhat *larger* (0.0033 and 0.0056 Å) than those from the $B_0$, with a smaller value for $R_N - R_C$ (0.0173 versus 0.0196 Å).





*4.3. Charge rearrangement at the nitrogens*

The agreement in the values found for $\theta_1$ and for $\theta_2$ by the two methods encourages us to treat them as reliable values for the torsional amplitudes. Therefore, we use them in eq. (2), along with the experimental results for $\chi_a$ from table 3, to obtain $\chi_0^d$ for the two $^{14}N$ of the dimer. This approach assumes that $\chi_0^d$ is not itself a function of the $\theta$. In this way, the averages for $\theta_n$ give $\chi_0^d(1)$ and $\chi_0^d(2)$ to be −4.4802 and −4.6029 MHz, respectively. For the free monomer, $\chi_0^m$ is −4.7091 MHz [10], so by defining

$$\Delta\chi_0 = \chi_0^d - \chi_0^m\,, \tag{8}$$

we find $\Delta\chi_0(1) = 0.2289$ and $\Delta\chi_0(2) = 0.1062$ MHz as the changes in quadrupole interaction constant produced by the charge rearrangement upon dimer formation.

These changes are 38% of the observed differences $\Delta\chi_a = \chi_a - \chi_0^m$; they compare favorably with the theoretical estimate of approximately half [3]. The charge redistribution effects themselves are quite small, 4.9% of $\chi_0^m$ for N(1) and only 2.3% for N(2). In making these estimates, the $\chi_a$ are known quite accurately so the uncertainties depend very largely upon those in $\theta_n$. The differences found in $\theta_n$ by the two methods lead to an uncertainty of about ±10% in $\Delta\chi_0$. With allowance for it, the charge redistribution effects account for 40 ± 5% of $\Delta\chi_a$.

Support for this analysis is provided by the $\chi_a$ values measured for N(1) and N(2) in the $DC^{14}N$–$HC^{15}N$ and $HC^{15}N$–$DC^{14}N$ dimers (table 3). Their use in eq. (2) along with the values given just above for $\chi_0^d(1)$ and $\chi_0^d(2)$ leads to torsional angles of 12.9 and 8.5° for DCN(1) and DCN(2). The ratios of the angles for $HC^{14}N$ versus $DC^{14}N$ are then 13.65/12.9 and 9.0/8.5, or 1.058 and 1.059. These ratios are in good agreement with the independently determined values 1.052 and 1.059 employed in section 4.4.

*4.4. Analysis of $\chi_D$ and r(C–D)*

Deuterium substitution has a much larger effect upon the moment of inertia for the monomer than $^{15}N$ or $^{13}C$ substitution, and its effects upon torsional motions in the dimer are correspondingly larger. We can estimate the torsional angles for DCN for the results, 13.65 and 9.0°, obtained for the HCN dimer. The reduction factor $(I_{DCN}/I_{HCN})^{1/4}$ is 1.0518. However, a somewhat larger factor of 1.0591 is indicated for $\theta_2$ from studies of $\chi$(N) in the dimers of acetylene, ethylene and $N_2$ with HCN/DCN, where charge rearrangement effects are negligible [8,11,12]. This leads to 13.0 and 8.5° for $\theta_1$ and $\theta_2$ of DCN in the dimers. In turn, these angles via eq. (2) and the experimental $\chi_a$(D) results in table 3, give values for $\chi_0^d$(D(1)) and $\chi_0^d$(D(2)) of 198 and 182 kHz.

Interpretation of these results is hampered a bit by some uncertainty in $\chi_0^m$, the deuterium quadrupole coupling constant in free DCN [10,13,14]. If we take its value to be 194.4(40) kHz, as is usually done, we conclude that the hydrogen bonding has little or no effect on $\chi_0^m$ for D(1), but causes a decrease of about 12 kHz (6%) for D(2), the deuterium in the hydrogen bond. Such decreases in $\chi$(D) with hydrogen bonding have been separated into two parts, one associated with elongation of the C–D bond and the other, all else. The elongation effect $\partial\chi/\partial r$ has been calculated to be −1260 kHz/Å for C–H [15]. Use of this value with the observed decrease of 12 kHz places an upper bound of 0.010 Å on elongation of the C–D (or C–H) bond in the HCN dimers.

In addition, the C–D bond length is shorter than C–H in the monomers [16]. The amount ranges from 0.0018 to 0.0046 Å depending upon which pairs of $B_0$ are employed to determine $r_0$. The average difference is 0.0028 Å. This difference persists in the dimers. For example, the $B_0$ values for the homodimers $(HCN)_2$ and $(DCN)_2$ can be used in eq. (1) with the $\theta$ values given above, to obtain the c.m. distance for each dimer. The $R$ found for $(DCN)_2$ is 0.0016 Å shorter than that for $(HCN)_2$. Similar effects occur in the HCN trimer.

**Acknowledgement**

Acknowledgement is made to the donors of the Petroleum Research Fund, administered by the American Chemical Society, for partial support of this research. The work was also supported by the National Science Foundation.

## References


[1] R.S. Ruoff, T. Emilsson, T.D. Klots, C. Chuang and H.S. Gutowsky, 41st Symposium on Molecular Spectroscopy, Columbus, OH (1986), Abstract TF13.

[2] K. Georgiou, A.C. Legon, D.J. Millen and P.J. Mjöberg, Proc. Roy. Soc. A399 (1985) 377.

[3] L.W. Buxton, E.J. Campbell and W.H. Flygare, Chem. Phys. 56 (1981) 399.

[4] A.J. Fillery-Travis, A.C. Legon, L.C. Willoughby and A.D. Buckingham, Chem. Phys. Letters 102 (1983) 126.

[5] M.R. Keenan, L.W. Buxton, E.J. Campbell, A.C. Legon and W.H. Flygare, J. Chem. Phys. 74 (1981) 2133.

[6] H.S. Gutowsky, T.D. Klots, C. Chuang, J.D. Keen, C.A. Schmuttenmaer and T. Emilsson, J. Am. Chem. Soc. 109 (1987), to be published.

[7] W. Gordy and R.L. Cook, Microwave molecular spectra (Interscience, New York, 1970).

[8] E.J. Goodwin and A.C. Legon, J. Chem. Phys. 82 (1985) 4434.

[9] E.F. Pearson, R.A. Creswell, M. Winnewisser and G. Winnewisser, Z. Naturforsch. 31a (1976) 1394.

[10] F. DeLucia and W. Gordy, Phys. Rev. 187 (1969) 58.

[11] P.D. Aldrich, S.G. Kukolich and E.J. Campbell, J. Chem. Phys. 78 (1983) 3521.

[12] S.G. Kukolich, W.G. Read and P.D. Aldrich, J. Chem. Phys. 78 (1983) 3552.

[13] Cited in: S.C. Wofsy, J.S. Muenter and W. Klemperer, J. Chem. Phys. 53 (1970) 4005.

[14] G. Cazzoli, C.D. Esposti and P.G. Favero, J. Phys. Chem. 84 (1980) 1756.

[15] H. Huber, J. Chem. Phys. 83 (1985) 4591.

[16] G. Winnewisser, A.G. Maki and D.R. Johnson, J. Mol. Spectry. 39 (1971).